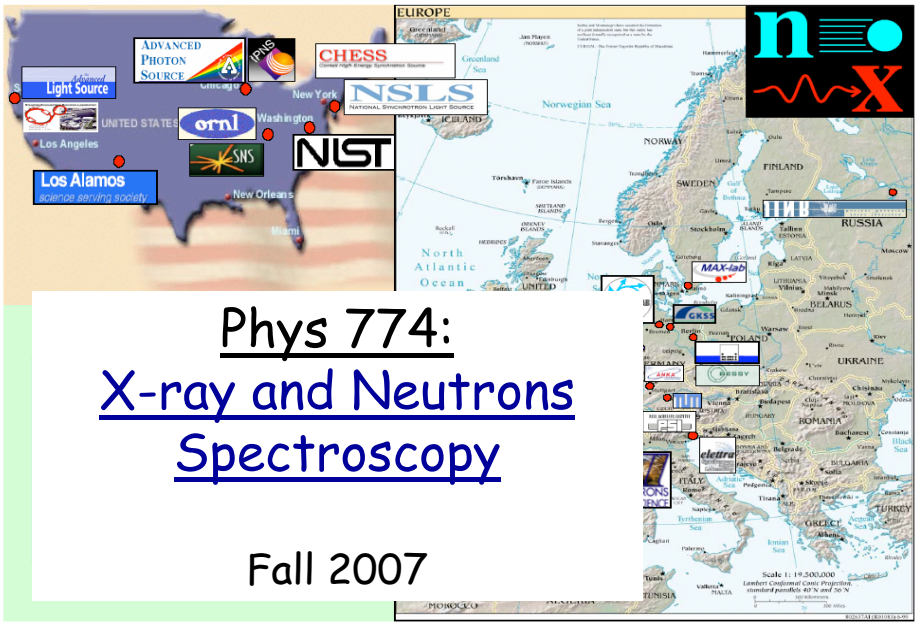

Phys 774:
X-ray and Neutrons Spectroscopy

Fall 2007

Optical Characterization in Industry, National Labs, and Academia

1. **Industrial Materials Characterization using Spectroscopic techiques**
2. **Multiuser facilities at National Labs**
3. **University Optical Labs**

Major suppliers of Spectroscopic Equipment (solutions)

JY Horiba

Bruker / Siemens

Sopra

Philips

Accent-Biorad

Spectra-Physics

Parts: Edmund Optics and CVI

Optical Characterization in Industry:

Materials and device structure characterization in a production line

1. **Thin films, coatings, multilayers**
2. **Composition and strain**
3. **Conductivity / resistance**
4. **Nanotechnology and nanoscale characterization**
5. **In situ characterization (on fly)**

Issues:

Maintanence

Speed

Interpretation and models

1. **FT-IR Reflectivity and Transmission** (IV)
2. **Raman Scattering (III-V)**
3. **Spectroscopic ellipsometry** (IV)
4. **Photoluminescence (III-V)**
5. **Micro-photoluminescence (III-V,IV)**
6. **X-ray diffraction (III-V)**
7. **X-ray fluorescence**
8. **E-beam spectroscopy**
9. **Imaging vs. Analythical characterization**

Optical Characterization in National Labs

New materials and ideas

1. **Emergent materials**
2. **New instrumentation / new techniques**
3. **Bio-optics**
4. **Nanomaterials**
5. **In situ characterization**

1. **Micro FT-IR Reflectivity and Transmission**
2. **Surface-enhanced Raman Scattering**
3. **Far-IR Spectroscopic ellipsometry** (IV)
4. **Near-field Photoluminescence (III-V)**
5. **Nano-scale X-ray diffraction (III-V)**
6. **X-ray fluorescence / X-ray standing waves**
7. **E-beam bio-imaging**

Goals: unique experiments with emergent materials

Examples of Optical Characterization in National Labs

New materials and ideas

Co-Localization of β-Amyloid Deposits and Metal Accumulation in Alzheimer's Disease

Beamline:
NSLS: U10B, X26A, X27A
APS: 13ID, 18ID

Technique:
Infrared Microspectroscopy
X-ray Fluorescence Microprobe

Researchers:
Q. Wang, T. P. Telivala, R. Smith, A. Lanzirotti, L. M. Miller (BNL), J. Miklossy (UBC)

Publication:
Lisa M. Miller, Qi Wang, Tejas P. Telivala, Randy J. Smith, Antonio Lanzirotti and Judith Miklossy. *Journal of Structural Biology, 155(1): 30-3, 2006*

Motivation: Alzheimer's disease (AD) is characterized by the misfolding and plaque-like accumulation of a naturally occurring protein, amyloid beta (Aβ) in the brain. This misfolding process has been associated with the binding of metal ions such as Fe, Cu, and Zn *in vitro*. The secondary structure of the amyloid plaques is imaged *in situ* using Fourier transform infrared microspectroscopy (FTIRM). The metal ion accumulation in the identical brain tissue is detected by synchrotron x-ray fluorescence (XRF) microprobe synchrotron. The aim is to spatially correlate the *in situ* metal distribution with the characteristic protein structure changes of amyloid plaques.

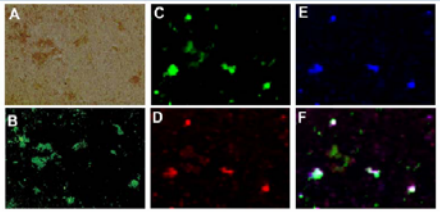

Figure 1. (A) Bright field and (B) Epifluorescence image of human AD tissue stained with Thioflavin S. (C) Single channel color FTIR correlation image of -sheet protein (green). (D) Single channel color SXRF microprobe image of Zn (red). (E) Single channel color SXRF microprobe image of Cu (blue). (F) The RGB correlation image.

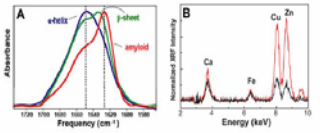

Figure 2 (A) Infrared spectra of Thioflavin-positive area (red) and Thioflavin-negative area (black) of AD tissue; FTIR spectrum of purified Aβ peptide in vitro is shown (green). (B) SXRF microprobe spectra from Thioflavin-positive area (red) and Thioflavin-negative area (black).

Examples of Optical Characterization in National Labs

New materials and ideas

Changes in Protein Structure and Distribution Observed at Pre-Clinical Stages during Scrapie Pathogenesis

Beamline: U10b

Technique: Infrared microspectroscopy

Researchers:
L.M. Miller, A. Kretlow, Q. Wang (BNL), M. Beekes, D. Naumann (Robert Koch-Inst., Berlin)

Publications:
1) A.Kretlow, Q. Wang, M. Beekes, D. Naumann, L.M. Miller. *Anal.Bioanal.Chem.* submitted

2) A. Kretlow, Q. Wang, J. Kneipp, P. Lasch, M. Beekes, L.M. Miller, D. Naumann. *Biochim. Biophys. Acta* **1758**: 948-59 (2006).

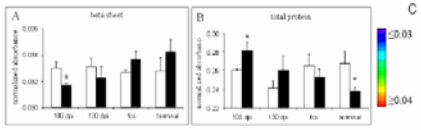

Motivation: Transmissible spongiform encephalopathies, such as scrapie, mad cow disease and Creutzfeldt-Jakob disease are fatal neurodegenerative disorders of the CNS and are characterized by the conversion of the α-helical rich normal prion protein into aggregates of its β-sheet rich conformer. To analyze the disease-related protein structural changes during scrapie pathogenesis directly in the tissue we investigated dorsal root ganglia of scrapie infected hamsters at different time points of the disease.

Results: Results showed clear changes in protein content, composition, and distribution as the disease progressed. At pre-clinical time points, the scrapie-infected animals exhibited a significant increase in protein expression, yet the β-sheet protein content was significantly lower than in controls. As the disease progressed, the β-sheet protein content increased near the cell membrane and in the cytoplasm of infected neurons, above the amount attributable to PrP^{Sc}. Subsequent immunostaining confirmed that this increase was at least partly due to the formation of PrP^{Sc}. At the terminal stage, the relative protein expression declined significantly, possibly due to degeneration and death of neurons. Based on these findings, we suggest that the pre-clinical stages of scrapie are characterized by an overexpression of proteins low in β-sheet content. As the disease progresses, PrP^{C} is converted to PrP^{Sc}, along with the conversion or replacement of other α-helical-rich proteins by β-sheet proteins. The dramatic changes in protein content and structure at pre-clinical time points emphasizes the need for identifying protein changes involved in early pathogenesis, which are important for understanding the disease and may provide a mechanism for early TSE diagnosis and treatment.

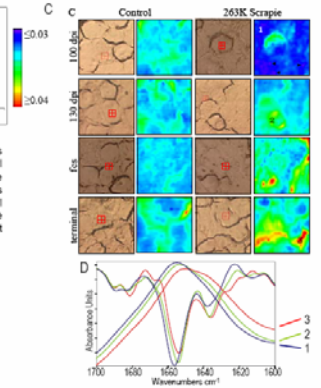

Mean values + average deviation for the (A) β-sheet and (B) total protein content for infected (black bars) and control (white bars) hamster dorsal root ganglia at the four investigated time points. Asterisks mark significant differences ($p<0.05$) between scrapie and control. (C) Photomicrographs of unstained cryo-sections (1st and 3rd columns) and corresponding FTIRM images (2nd and 4th columns) of the β-sheet distribution for control (left) and infected (right) ganglia at different time points. Areas exhibiting extremely low β-sheet at 100 dpi are indicated by arrowheads. (D) Original and 2nd derivative spectra of areas indicated by numbers in the chemical maps. Red square in photomicrographs: 10x10 µm.

Examples of Optical Characterization in National Labs

New materials and ideas

Compositional Changes Observed in the Calcified Cartilage and Subchondral Bone in a Monkey Model of Osteoarthritis

Beamline: U10B

Technique: Infrared Microspectroscopy

Researchers:
Meghan E. Ruppel, Lisa M. Miller (BNL-NSLS); Cathy S. Carlson (Univ. of Minnesota)

Publications:
L.M. Miller, J. Tetenbaum Novatt, D. Hamerman, C.S. Carlson. Bone, 35 (2): 498-506 (2004).

M.E. Ruppel, C.S. Carlson, L.M. Miller. *In preparation*

Motivation: Osteoarthritis (OA) can be a debilitating disease that is characterized by fibrillation and calcification of the articular cartilage and thickening of the subchondral bone. In the present study, the chemical makeup of both the calcified cartilage and subchondral bone were studied in a primate model of OA. Mid-coronal sections of proximal tibia from cynomolgus monkeys were examined. Synchrotron-assisted Fourier transform infrared microscopy (FTIRM) was used to determine the level of mineralization (mineral/protein ratio), carbonate accumulation (carbonate/phosphate ratio), and collagen fibril orientation (amide I/II band ratio) as a function of tissue compartment and OA severity.

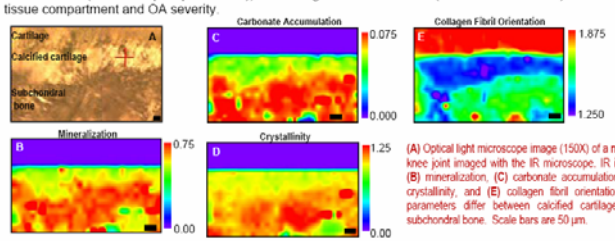

(A) Optical light microscope image (150X) of a normal knee joint imaged with the IR microscope. IR image (B) mineralization, (C) carbonate accumulation, (D) crystallinity, and (E) collagen fibril orientation. All parameters differ between calcified cartilage and subchondral bone. Scale bars are 50 µm.

Results: Results showed that the level of mineralization ($p=0.0431$) and carbonate accumulation ($p<0.0001$) were significantly higher in subchondral bone when compared to calcified cartilage. The amide I/II ratio was also significantly different between the subchondral bone and calcified cartilage, suggesting differences in collagen organization between the two tissue compartments. As a function of OA severity, the mineralization level of the calcified cartilage increased ($p=0.0037$), but the subchondral bone remained unchanged. The collagen orientation was not affected by OA severity. Compositional differences between calcified cartilage and subchondral bone suggest subchondral bone is older, more mature tissue. Additionally compositional changes that are observed as a function of OA severity are consistent with the progression of a "mineralization front" where endochondral ossification occurs and calcified cartilage is replaced by subchondral bone. These findings indicate that calcified cartilage and subchondral bone have distinctly different collagen structure and mineral composition that are affected by OA severity and could increase stress on the afflicted joints.

Synchrotron- and Neutron Scattering Places

How to get an access to multi-user facilities at National Labs

Need ideas

1. Select Facility (Synchrotron, Observatiry, Neutron source, ...)
2. Register as a user
3. Write a proposal. Remember that Proposals become „Public Information“
4. Schedule time for experiment
5. Pass safety training
6. Arrive to Facility and carry out experiments exactly how it is described in your proposal
7. Write a paper
8. Start this process over

HW: write a 2-page proposal for any experiment

Follow guidelines for proposal writing at any Facility, e.g, CHESS

OUTLINE

1. X-ray Spectroscopy

   X-ray radiation. Sources of X-rays, Detection of X-rays

   Primary techniques: Fluorescence, Diffraction, Scattering

   Instrumentation: Diffractometers, detectors

   Applications

2. Neutrons Spectroscopy

   Sources, Detectors

   Techniques: diffraction and Inelastic scattering

   Instrumentation and Applications

Discovery of X-rays

Wilhelm Conrad Röntgen 1845-1923

1895: Discovery of X-Rays

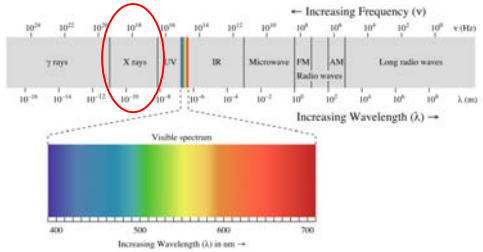

Nobel Prizes for Research with X-Rays

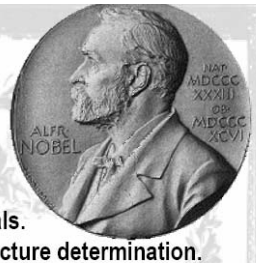

1901 W. C. Röntgen in Physics for the discovery of x-rays.
1914 M. von Laue in Physics for x-ray diffraction from crystals.
1915 W. H. Bragg and W. L. Bragg in Physics for crystal structure determination.
1917 C. G. Barkla in Physics for characteristic radiation of elements.
1924 K. M. G. Siegbahn in Physics for x-ray spectroscopy.
1927 A. H. Compton in Physics for scattering of x-rays by electrons.
1936 P. Debye in Chemistry for diffraction of x-rays and electrons in gases.
1962 M. Perutz and J. Kendrew in Chemistry for the structure of hemoglobin.
1962 J. Watson, M. Wilkins, and F. Crick in Medicine for the structure of DNA.
1979 A. McLeod Cormack and G. Newbold Hounsfield in Medicine for computed axial tomography.
1981 K. M. Siegbahn in Physics for high resolution electron spectroscopy.
1985 H. Hauptman and J. Karle in Chemistry for direct methods to determine x-ray structures.
1988 J. Deisenhofer, R. Huber, and H. Michel in Chemistry for the structures of proteins that are crucial to photosynthesis.

OTHER USE of X-RAYS

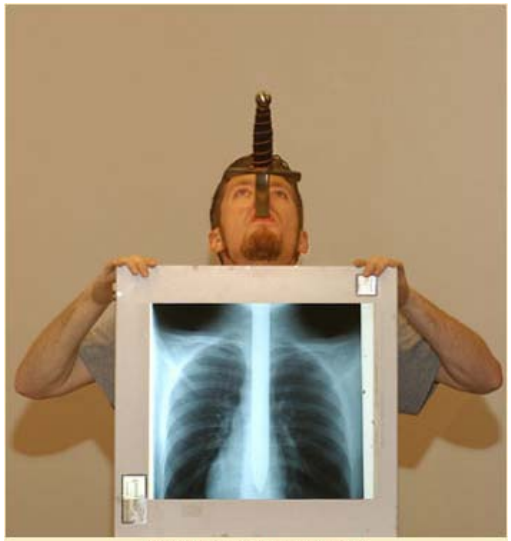

Roderick Russell - Frontal X-Ray
Photo Courtesy of Ellison Badger

Wavelength and the size of observable objects

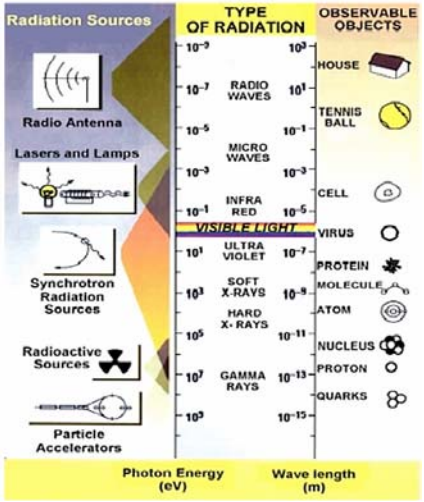

	Scatterers (spacings)	Radiation (typical dimension)
Electron-beam (3.7 pm for 100 keV)	Ink dots in newsprint (0.1 mm)	
Light (520 nm for green)	Raindrops (10 mm)	
X-ray (0.154 nm for Cu Kα)	Row of parked cars (3 m)	
Sound (1.26 m at middle C)	Precipitates in alloys (100 nm)	
Thermal radiation (0.1 m typical)	Atoms in crystals (0.1 nm)	

Wavelength ≈ Object Size ≈ Angstroms for Condensed Matter Research

$$\lambda[\text{Å}] = \frac{12.398}{E_{ph}[\text{keV}]}$$

The most important information arises when the wavelength of the radiation is similar to, or smaller than, the size of the spacing between the objects being studied.

Interaction of Electrons, X-rays, and Neutrons with matter

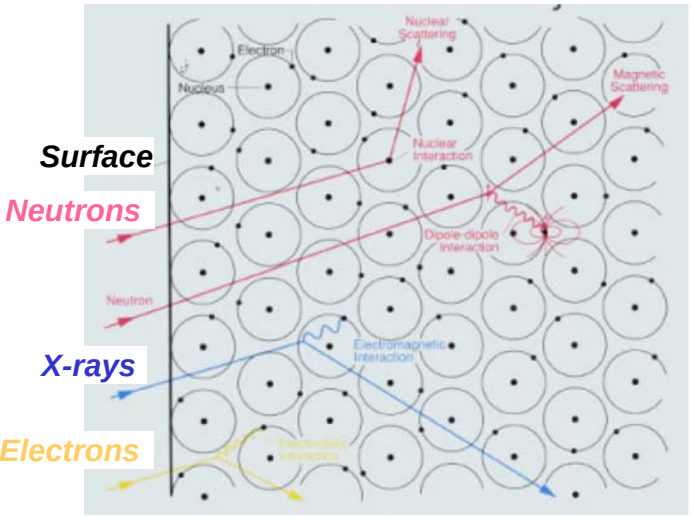

- Neutrons interact with atomic nuclei via very short range (~fm) forces.
- Neutrons also interact with unpaired electrons via a magnetic dipole interaction.

Neutrons vs. x-rays

- Whereas neutrons interact primarily by the strong force, x-rays interact by scattering from electrons.
- The interaction of neutrons with nuclei has the advantage that neutrons can see small atoms (the scattering power for neutrons varies almost randomly for neutrons, as compared to x-rays where it goes like Z^2).
- Neutrons are therefore well-suited to study low-Z atomic structures.

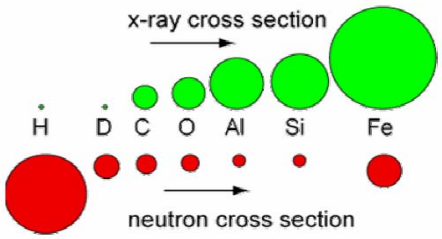

This shows how the cross-section, which is related to the size of the Bragg peaks, varies for x-rays (where it increases for increasing size of the atoms, and therefore the number of electrons), compared to neutrons (where it is governed by nuclear interactions – almost random).

Sources of X-rays

- X-rays in conventional labs are usually produced by the inverse photoelectric effect (ie. Electrons are accelerated to a target metal, and when they slow down they produce x-ray radiation).
- However, you can produce extremely bright x-rays from synchrotron radiation – accelerate charged particles to very high speeds, and then bend their trajectories using electric and magnetic fields.
- At every 'bend', the charged particles are accelerated, and they give off x-ray radiation.

The Canadian Light Source
(Saskatoon, Saskatchewan)
http://www.cls.usask.ca/

"Conventional x-rays"

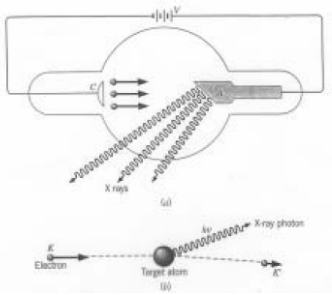

Synchrotron x-rays

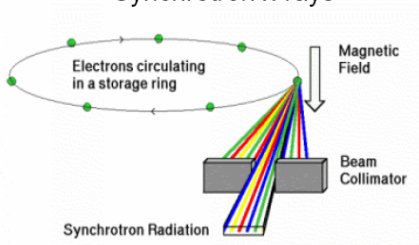

X-ray tubes

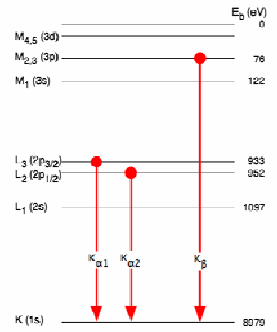

Electronic transitions

X-ray tube

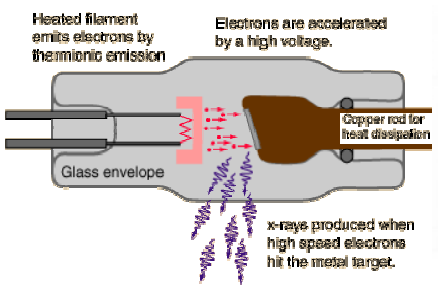

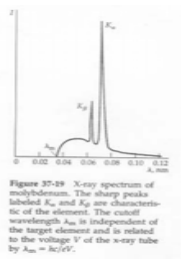

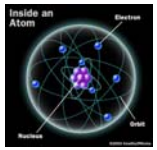

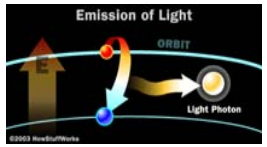

X-ray K-series spectral line wavelengths (nm) for some common target materials.[5]

Target	Kβ₁	Kβ₂	Kα₁	Kα₂
Fe	0.17566	0.17442	0.193604	0.193998
Ni	0.15001	0.14886	0.165791	0.166175
Cu	0.139222	0.138109	0.154056	0.154439
Zr	0.070173	0.068993	0.078593	0.079015
Me	0.063229	0.062099	0.070930	0.071359

Synchrotron Radiation

Synchrotron radiation

Synchrotron Radiation produced by relativistic electrons in accelerators (since 1947)

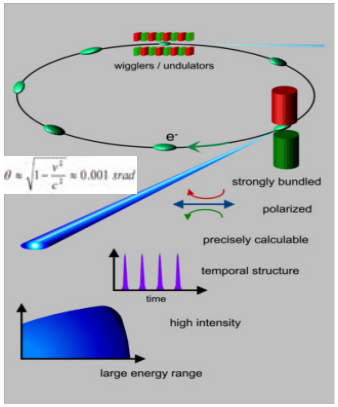

Natural Synchrotron Radiation

Stars and Galaxies

Synchrotron Radiation

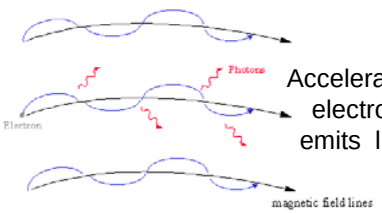

Accelerating electron emits light

Synchrotron radiation has a number of unique properties:
- High brightness: synchrotron radiation is extremely intense (hundreds of thousands of times higher than conventional X-ray tubes) and highly collimated.
- Wide energy spectrum: synchrotron radiation is emitted with a wide range of energies, allowing a beam of any energy to be produced.
- Synchrotron radiation is highly polarised.
- It is emitted in very short pulses, typically less that a nano-second (a billionth of a second)

HOW CAN WE SELECT A WAVELENGTH

Usually, you get a broad band of x-ray radiation from these sources. To choose a wavelength (even from a conventional source), you often find a crystal with a strong Bragg reflection and use it as a monochromator. Since the crystal will only reflect x-rays at one wavelength (or multiples of that wavelength – think about why), this method is very effective.

source

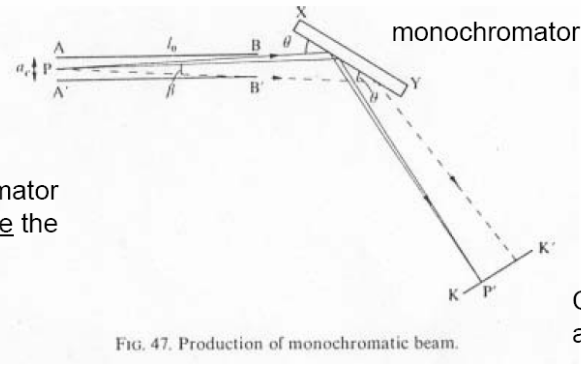

monochromator

A monochromator is used before the sample.

Crystal you are measuring

FIG. 47. Production of monochromatic beam.

Closer look at the properties of Synchrotron Radiation

Synchrotron X-rays

Advantages

1) λ_n - Interatomic Spacing
2) High Brilliance of X-ray Sources - High Resolution; Small Samples; High Degree of Coherence
3) No Kinematic Restrictions (E,Q uncoupled)
4) No Restriction on Energy Transfer that Can Be Studied

Disadvantages

1) Strong Absorption for Lower Energy Photons
2) Little Contrast for Hydrocarbons or Similar Elements
3) Weak Scattering from Light Elements
4) Radiation Damage to Samples

Synchrotrons

- Usually, you need very large facilities to produce these beams.
- The ESRF is located at the meeting of 2 rivers in Grenoble, France.

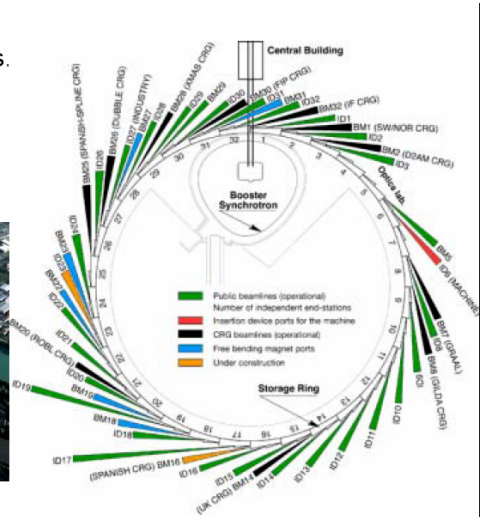

The European Synchrotron Radiation Facility

Brightness & Fluxes for Neutron & X-Ray Sources

	Brightness $(s^{-1}m^{-2}ster^{-1})$	dE/E (%)	Divergence $(mrad^2)$	Flux $(s^{-1}m^{-2})$
Neutrons	10^{15}	2	10×10	10^{11}
Rotating Anode	10^{20}	0.02	0.5×10	5×10^{14}
Bending Magnet	10^{27}	0.1	0.1×5	5×10^{20}
Undulator (APS)	10^{33}	10	0.01×0.1	10^{24}

Progress with Brilliance of Synchrotron Radiation

Why Synchrotron-radiation ?

Intensity !!!

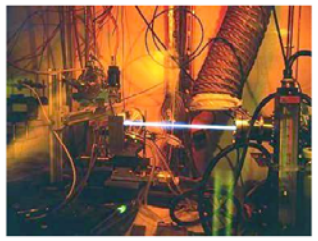

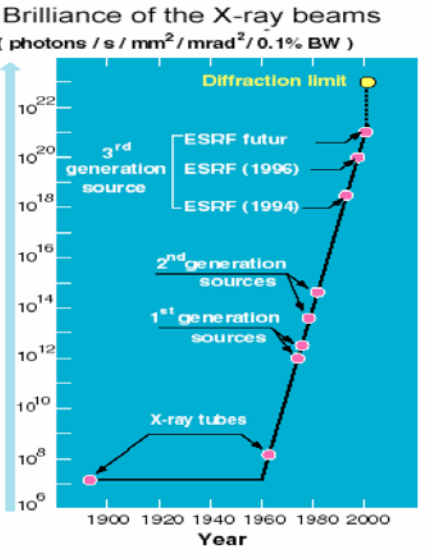

EXAMPLES of SYNCHROTRON RADIATION HIGHLIGHTS

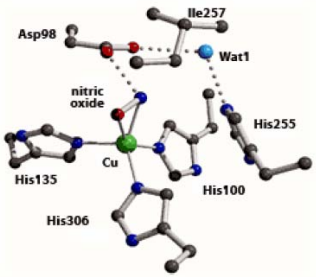

Complicated chemical structures

Stanford Synchrotron Radiation Lab
(http://www-ssrl.slac.stanford.edu/)

Bright x-rays can see
Low Z atoms (like hydrogen)
- Structure of complicated biomolecules

EXAMPLES of SYNCHROTRON RADIATION HIGHLIGHTS

You can use x-rays like an electron microscope
(this isn't diffraction)

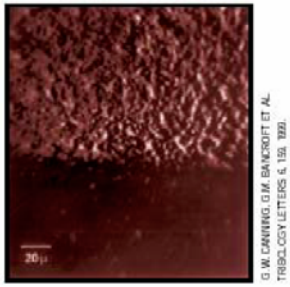

Surface of a silicon composite

Canadian Light Source

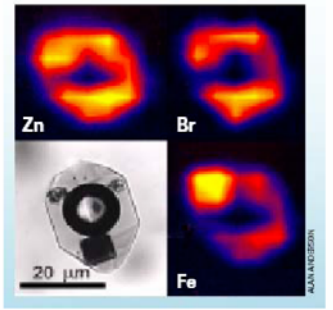

Elemental Analysis:
Targets absorb x-rays at certain energy levels, so by tuning the beam To these energy levels and watching how many xrays are absorbed, you can see what materials are made of.

DIFFRACTION vs. SCATTERING

SCATTERING of X-rays

Scattering Geometry: General Consideration

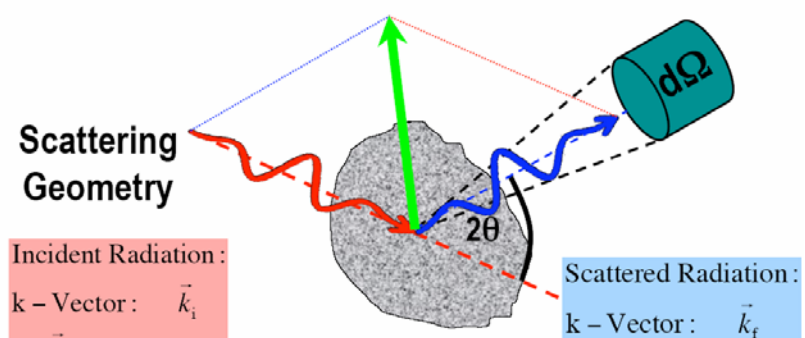

Incident Radiation:
k – Vector: $\vec{k}_i$
$|\vec{k}_i| = 2\pi/\lambda$
Energy: E_i
Polarization: $\vec{p}_i$

Scattered Radiation:
k – Vector: $\vec{k}_f$
Energy: E_f
Polarization: $\vec{p}_f$

Wavevector Transfer:
$\vec{q} = \vec{k}_f - \vec{k}_i$
Energy Transfer:
$\Delta E = E_f - E_i = \hbar\omega$
Polarization:
$\vec{p}_i \rightarrow \vec{p}_f$

For X-Rays:
$\Delta E << E_f, E_i$
$\Rightarrow \quad |\vec{q}| = 2k_i \sin(2\theta/2)$

Scattering Cross Section

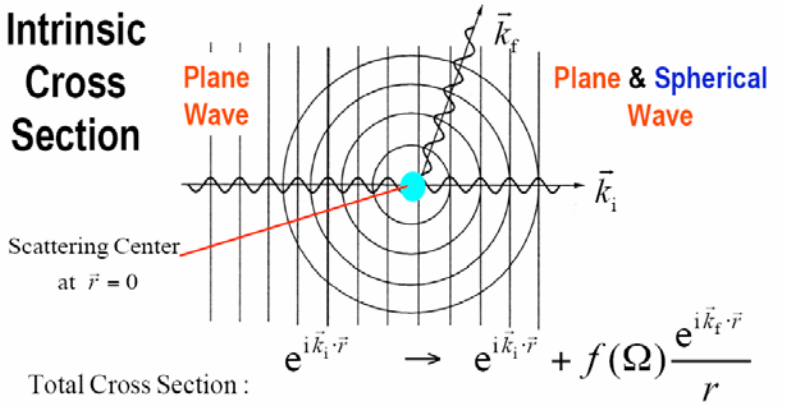

Total Cross Section:

$$\sigma = \iint \left(\frac{d\sigma}{d\Omega}\right)_0 d\Omega$$

$$\sigma = \int_0^{2\pi}\int_0^{\pi} |f(\vartheta,\phi)|^2 \sin\vartheta \, d\vartheta \, d\phi$$

$$\left(\frac{d\sigma}{d\Omega}\right)_0 = |f(\Omega)|^2$$

Scattering Cross Section

Intrinsic Cross Section: X-Rays

$$\vec{E}_{in} = \vec{E}_0 e^{i(\vec{k}\cdot\vec{r}-\omega t)}$$

$$E_{rad}(R,t) = \frac{e}{4\pi\varepsilon_0 c^2 R}\ddot{x}(t - R/c)$$

$$\ddot{x}(t - R/c) = -\frac{e}{m}\alpha(\omega)E_{in}e^{i\omega R/c}\cos\psi$$

$$\frac{E_{rad}(R,t)}{E_{in}} = -r_0\alpha(\omega)\frac{e^{ikR}}{R}\cos\psi$$

Thomson Scattering Length of the Electron (classical electron radius):

$$r_0 = \frac{e^2}{4\pi\varepsilon_0 mc^2} = 2.82\times10^{-15}\,\text{m}$$

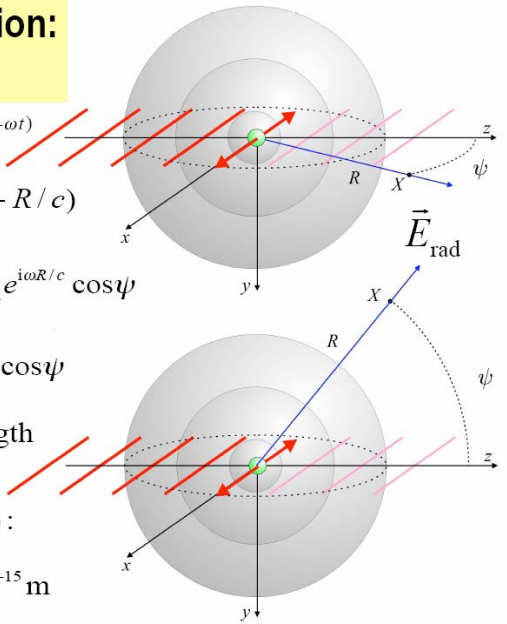

Scattering by individual atoms
(Mutual interference between scattered rays gives diffraction pattern)

Scattering from atom

Consider single electron. Plane wave $E_{in} = E_0 e^{i(\mathbf{k}\cdot\mathbf{r}-\omega t)}$ $k = |\mathbf{k}| = \frac{2\pi}{\lambda}$

Scattered field: $E' = f_e \frac{E_0}{R} e^{i(kR-\omega t)}$ f_e – *scattering length of electron*
R – radial distance

Two electrons: $E' = f_e \frac{E_0}{R} e^{ikR}\left[1 + e^{i\Delta\mathbf{k}\cdot\mathbf{r}}\right]$

or, more generally $E' = f_e \frac{E_0}{R} e^{ikR}\left[e^{i\Delta\mathbf{k}\cdot\mathbf{r}_1} + e^{i\Delta\mathbf{k}\cdot\mathbf{r}_2}\right]$

many electrons: $E' = f_e \frac{E_0}{R} e^{ikR}\sum_l e^{i\Delta\mathbf{k}\cdot\mathbf{r}_l}$

similar to single electron with $f = f_e \sum_l e^{i\Delta\mathbf{k}\cdot\mathbf{r}_l}$

intensity: $I \sim |f|^2 = f_e^{\,2} \left| \sum_l e^{i\Delta\mathbf{k}\cdot\mathbf{r}_l} \right|^2$

this is for coherent scatterers. If random then $I \sim N f_e^{\,2}$

Scattering length of electron: $f_e = \left[\left(1 + \cos^2 2\theta\right)/2 \right]^{1/2} r_e$

classical electron radius $r_e = \dfrac{1}{4\pi\varepsilon_0} \dfrac{e^2}{mc^2} \approx 2.8 \times 10^{-15}$ m

In atom, $f_e \sum_l e^{i\Delta\mathbf{k}\cdot\mathbf{r}_l} \rightarrow f_e \int n(\mathbf{r}) e^{i\Delta\mathbf{k}\cdot\mathbf{r}_l} d^3r$

$n(\mathbf{r})$ – electron density

$f_a = \int n(\mathbf{r}) e^{i\Delta\mathbf{k}\cdot\mathbf{r}_l} d^3r$ ***- atomic scattering factor (form factor)***

Atomic scattering factor (dimensionless) is determined by electronic distribution.

If $n(\mathbf{r})$ is spherically symmetric, then

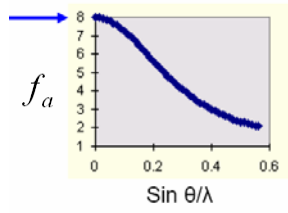

$$f_a = \int_0^{r_0} 4\pi r^2 n(r) \frac{\sin(\Delta k \cdot r)}{\Delta k \cdot r} dr$$

in forward scattering $\Delta k = 0$ so $f_a = 4\pi \int r^2 n(r) dr = Z$

Z - total number of electrons

Atomic factor for forward scattering is equal to the atomic Z number

(all rays are in phase, hence interfere constructively)

Scattering Cross Section

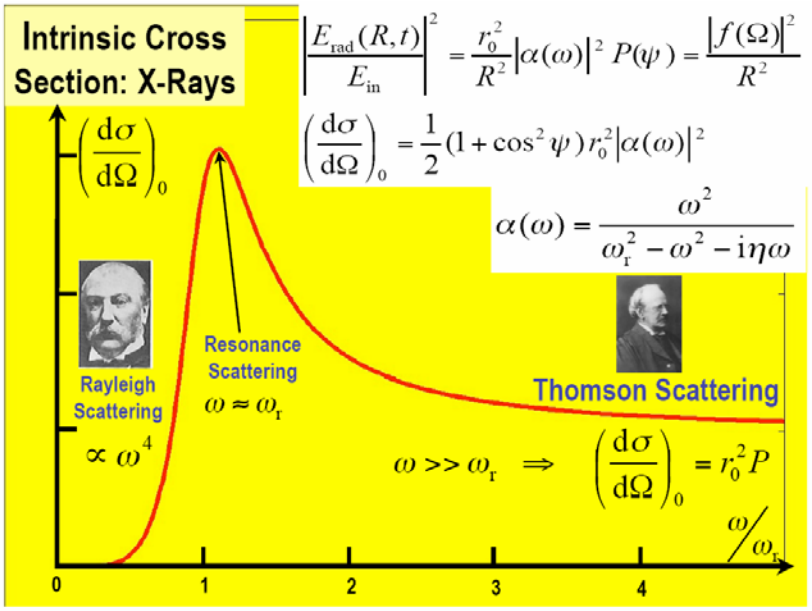

What we can measure?

Adding up phases at the detector of the wavelets scattered from all the scattering centers in the sample:

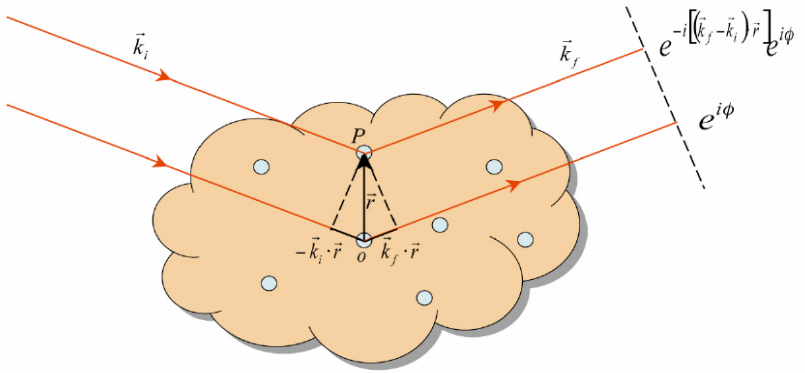

Scattering

X-rays

$$\frac{d\sigma}{d\Omega} = r_0^2 \frac{[1 + \mathrm{Cos}^2(2\theta)]}{2} S(\mathbf{q})$$

$$S(\mathbf{q}) = \langle \Sigma_{ij} \exp[-i\mathbf{q}.(\mathbf{r}_i - \mathbf{r}_j)] \rangle$$

$\{\mathbf{r}_i\}$ == electron positions.

$\Sigma_i \exp[-i\mathbf{q}.\mathbf{r}_i] = \rho_{el}(\mathbf{q})$ Fourier Transform of electron density

And, for x-rays, $S(\mathbf{q}) = \langle \rho_{el}(\mathbf{q}) \rho_{el}^*(\mathbf{q}) \rangle$

Scattering

If electrons are bound to atoms centered on nuclei at $\mathbf{R}_i$

$$\rho_{el}(\mathbf{r}) = \Sigma_i f_{el}(\mathbf{r} - \mathbf{R}_i)$$

$$\rho_{el}(\mathbf{q}) = \int d\mathbf{r} \exp[-i\mathbf{q}.\mathbf{r}] \Sigma_i f_{el}(\mathbf{r} - \mathbf{R}_i)$$

$$= \Sigma_i \{ \int d\mathbf{r} \exp[-i\mathbf{q}.(\mathbf{r} - \mathbf{R}_i)] f_{el}(\mathbf{r} - \mathbf{R}_i) \} \exp[-i\mathbf{q}.\mathbf{R}_i]$$

$$= f(\mathbf{q}) \Sigma_i \exp[-i\mathbf{q}.\mathbf{R}_i]$$

$$= f(\mathbf{q}) \rho_N(\mathbf{q})$$

$f(\mathbf{q})$ is called the Atomic Form Factor

Scattering

X-rays

$f = f_0 + \Delta f' + i\Delta f''$

"Scattering factor" $= Zf(q)$

"anomalous" big at edges

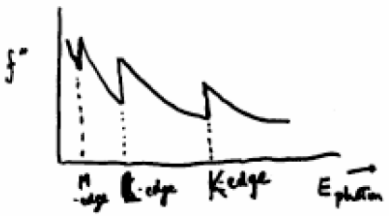

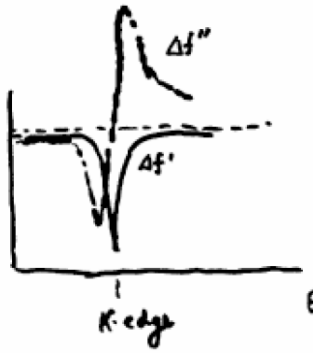

$$\Delta f'(E) = 2\pi \int \frac{\Delta f''(E')}{E - E'} dE'$$

"Kramers-Kronig Dispersion Relations

Scattering

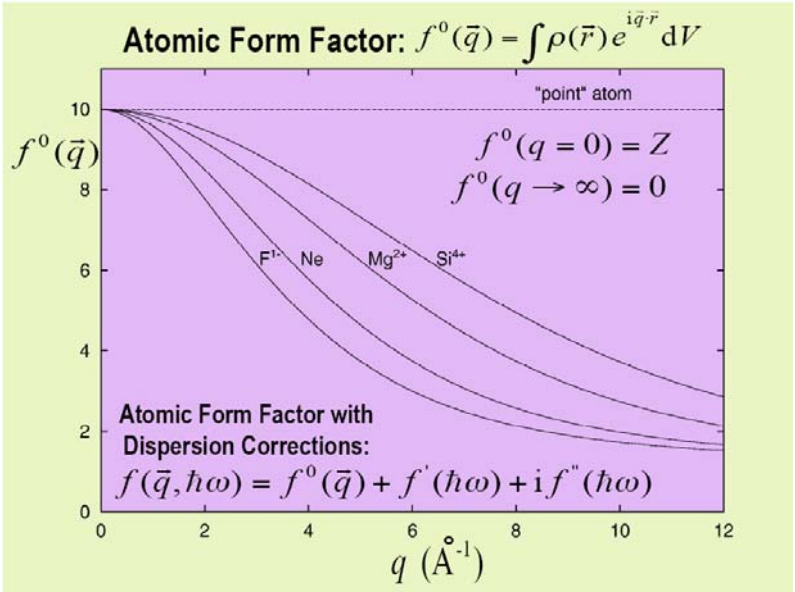

Scattering Length of a Molecule

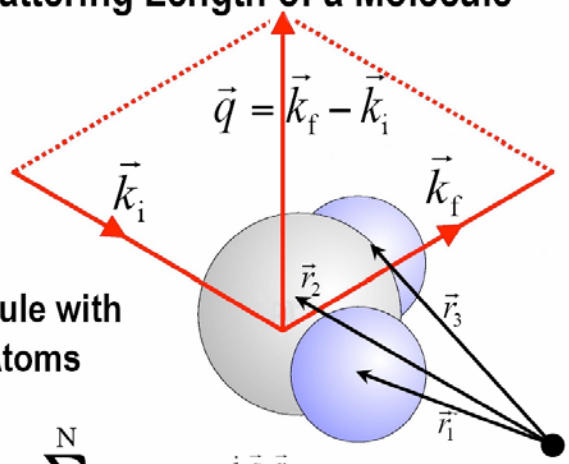

$$F_{mol.}(\vec{q}) = \sum_{j=1}^{N} f_j(\vec{q})\, e^{-i\,\vec{q}\cdot\vec{r}_j}$$

Example: CF_4 - Molecule

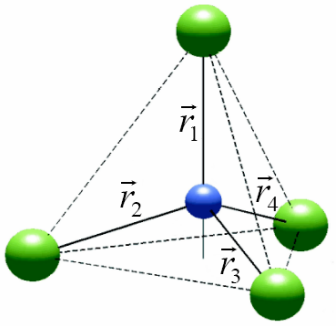

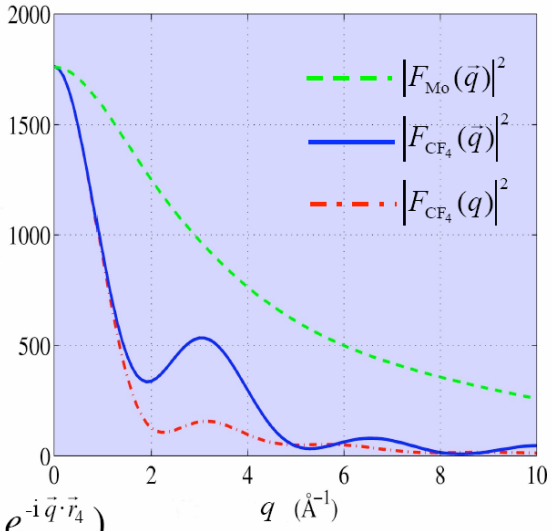

$$F_{CF_4}(\vec{q}) = f_C(\vec{q}) + f_F(\vec{q})\,(e^{-i\,\vec{q}\cdot\vec{r}_1} + e^{-i\,\vec{q}\cdot\vec{r}_2} + e^{-i\,\vec{q}\cdot\vec{r}_3} + e^{-i\,\vec{q}\cdot\vec{r}_4})$$

Applications of inelastic X-ray scattering: probing lattice vibrations (similar to Raman scattering)

Inelastic X-ray scattering

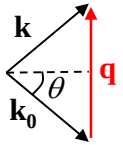

$$\mathbf{k} = \mathbf{k}_0 \pm \mathbf{q} \qquad \hbar\omega = \hbar\omega_0 \pm \hbar\Omega(\mathbf{q})$$

$$q = 2k_0 \sin\theta = 2n\frac{\omega_0}{c}\sin\theta$$

assumed $\Omega(\mathbf{q}) << \omega_0$
- true for x-rays:
$\hbar\Omega < 100$ meV; $\hbar\omega_0 \sim 10^4$ eV
n – index of refraction

measuring $\omega - \omega_0$ and $\sin\theta$ one can determine dispersion $\Omega(\mathbf{q})$

main disadvantage – difficult to measure $\omega - \omega_0$ accurately

This difficulty can be overcome by use of ***neutron scattering***

Energy of "thermal" neutrons is comparable with $\hbar\Omega$ (80 meV for $\lambda \approx 1$Å)

Inelastic X-ray scattering in GaN

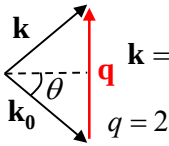

$$\mathbf{k} = \mathbf{k}_0 \pm \mathbf{q} \qquad \hbar\omega = \hbar\omega_0 \pm \hbar\Omega(\mathbf{q})$$

$$q = 2k_0 \sin\theta = 2n\frac{\omega_0}{c}\sin\theta$$

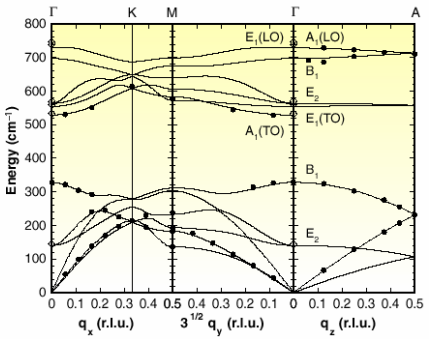

Phonon dispersion of wurtzite GaN (filled circles: IXS data; solid lines: ab initio lattice-dynamical calculation.

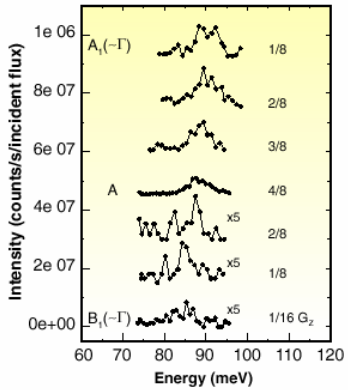

IXS spectra of wurtzite GaN along Γ-A. Values of q_z (in units of $G_z = 2\pi/c$) are given next to each spectrum.

Scattering from crystal

crystal scattering factor: $f_{cr} = \sum_l e^{i\Delta\mathbf{k}\cdot\mathbf{r}_l} = \sum_l f_{al} e^{i\Delta\mathbf{k}\cdot\mathbf{R}_l}$

$\mathbf{R}_l$ - position of l^{th} atom, f_{al} - corresponding atomic factor

rewrite $f_{cr} = F \cdot S$

where $F = \sum_j f_{aj} e^{i\Delta\mathbf{k}\cdot\mathbf{s}_j}$ - *structure factor* of the basis, summation over the atoms in unit cell

and $S = \sum_l e^{i\Delta\mathbf{k}\cdot\mathbf{R}_l^c}$ - lattice factor, summation over all unit cells in the crystal

Where $\mathbf{R}_l = \mathbf{R}_l^c + \mathbf{s}_j$

Since $\Delta\mathbf{k} = \mathbf{G}$, the lattice factor becomes $S = \sum_l e^{i\mathbf{G}\cdot\mathbf{R}_l^c} = \sum_l e^{i2\pi m} = N$

Then scattering intensity $I \sim |f_{cr}|^2$ where $f_{cr} = F \cdot N = N \sum_j f_{aj} e^{i\mathbf{G}\cdot\mathbf{s}_j}$

$\mathbf{G} = \mathbf{G}_{\text{hkl}} = h\mathbf{b}_1 + k\mathbf{b}_2 + l\mathbf{b}_3$ if $\mathbf{s}_j = u_j\mathbf{a}_1 + v_j\mathbf{a}_2 + w_j\mathbf{a}_3$

Then $F = \sum_j f_{aj} e^{i(u_j\mathbf{a}_1 + v_j\mathbf{a}_2 + w_j\mathbf{a}_3)(h\mathbf{b}_1 + k\mathbf{b}_2 + l\mathbf{b}_3)} = \sum_j f_{aj} e^{2\pi i(hu_j + kv_j + lw_j)}$

structure factor

Example: structure factor of bcc lattice (identical atoms)

structure factor $F = \sum_j f_{aj} e^{2\pi i(hu_j + kv_j + lw_j)}$

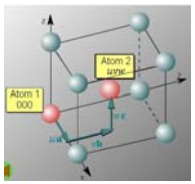

Two atoms per unit cell: $\mathbf{s}_1 = (0,0,0)$; $\mathbf{s}_2 = a(1/2,1/2,1/2)$

$$F = f_a\left[1 + e^{\pi i(h+k+l)}\right]$$

$\Rightarrow F=2f_a$ if $h+k+l$ is even, and $F=0$ if $h+k+l$ is odd

Diffraction is absent for planes with odd sum of Miller indices

---

For allowed reflections in fcc lattice *h,k,and l are all even or all odd*

4 atoms in the basis.

What about simple cubic lattice ?

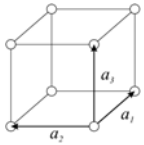

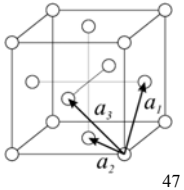

BCC structure

Consider the bcc lattice with single atoms at each lattice point, its unit cell can be reduced to two identical atoms. Atom 1 is at 000 with scattering factor f, and atom 2 is at ½½½ with a scattering factor f.

Have a go! Click on the animation opposite to illustrate the bcc unit cell.

The structure factor for the bcc unit cell is therefore:

$\mathbf{F} = f + f\exp(2\pi i(\frac{h}{2} + \frac{k}{2} + \frac{l}{2}))$

$= f(1 + \exp(\pi i(h + k + l)))$

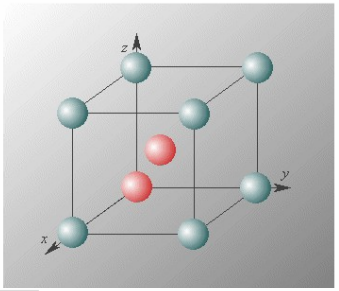

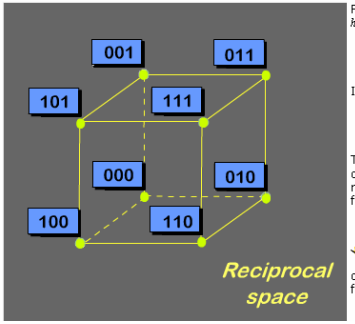

For diffraction from a plane where the sum of $h+k+l$ is odd, the second term is -1, so

$\mathbf{F}_{hkl\text{odd}} = f(1-1) = 0$

If $h+k+l$ is even, the second term is +1, so

$\mathbf{F}_{hkl\text{even}} = f(1+1) = 2f$

Thus, diffractions from bcc planes where $h+k+l$ is odd are of zero intensity. They are forbidden reflections. These reflections are usually omitted from the reciprocal lattice.

Have a go! Click on the animation opposite to illustrate the forbidden reflections from the bcc unit cell.

Structure factor of the BCC lattice

- What does this mean? Metallic sodium, for example, is BCC. The diffraction pattern does not contain lines such as (100), (300), (111), etc. – whenever the sum of integers hkl is odd. However, there are lines such as (200), (110), (222), etc.
- The physical reason is that reflections with $h+k+l$ = odd refer to planes of atoms where the rays are out of phase by π, so that each ray, from plane to plane, cancels out the next ray, and the net intensity is zero.
- An example: (100) reflection in the BCC cell:

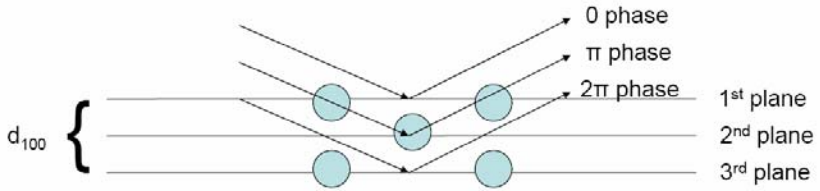

Structure factor of the FCC lattice

- For the FCC lattice, we have the basis (identical atoms at both positions):

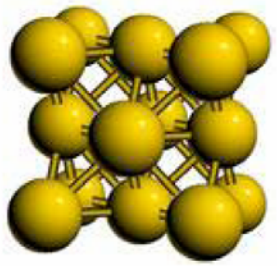

$x_1 = 0\ y_1 = 0\ z_1 = 0$
$x_2 = 0\ y_2 = ½\ z_2 = ½$
$x_3 = ½\ y_3 = 0\ z_3 = ½$
$x_4 = ½\ y_4 = ½\ z_4 = 0$

- So, this means that $F(h,k,l)$:

$$F(h,k,l) = f[1+\exp(-i\pi(h+k)+\exp(-i\pi(h+l)+\exp(-i\pi(k+l)]$$

- Therefore, if all the indices are even integers, or all are odd $F(h,k,l)$ = 4f. If 1 is even. and 2 are odd, then F = 0. If 1 is odd, and 2 are even, then F is zero. This means that no reflections can occur for which the indices are partly even and partly odd.

Structure factor of the FCC lattice

- Nickel has an FCC structure:

All even (hkl) or All odd (hkl)

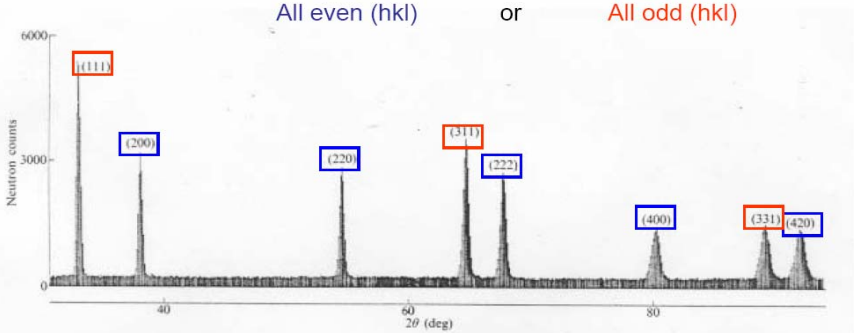

FIG. 58. A section of a powder diffraction pattern for nickel at a wavelength of 1·14 Å recorded on the PANDA diffractometer at A.E.R.E.-Harwell using a germanium monochromator. Counts are made at intervals of 0·1° of 2θ. (Courtesy of R. F. Dyer.)

Note: There are no reflections with mixtures of odd and even indices (eg. (110))

Structure factor of the SC lattice

- The structure factor F does not have to be real, because the intensity of the x-ray goes like $F \cdot F$ However, $F \cdot F$ must be real.
- For a simple cubic lattice, the structure factor is easy to calculate:

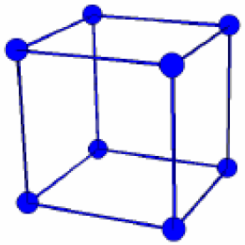

The basis is one atom, at (0, 0, 0).
(This will produce all the atoms in the unit cell by translation)

$$F(h,k,l) = f(\exp 0) = 1$$

This means all of the reflections where $\Delta\vec{k} = \vec{G}$ are allowed (so we see all reflections of the form (hkl), eg. (100), (110), any combination of integers). We will see that this is not true for the BCC and FCC lattice

Structure Compound: Calculation

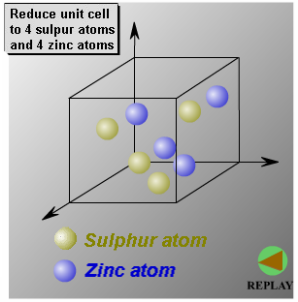

Structure factor calculation

Consider a general unit cell for this type of structure. It can be reduced to 4 atoms of type A at 000, 0 ½ ½, ½ 0 ½, ½ ½ 0 i.e. in the fcc position and 4 atoms of type B at the sites ¼¼¼ from the A sites. This can be expressed as:

$$\mathbf{F} = \{f_A + f_B e^{\frac{\pi}{2}(h+k+l)}\}\mathbf{F}_{fcc}$$

The structure factors for this structure are:

$\mathbf{F} = 0$ if h, k, l mixed (just like fcc)
$\mathbf{F} = 4(f_A \pm if_B)$ if h, k, l all odd
$\mathbf{F} = 4(f_A - f_B)$ if h, k, l all even and $h+k+l = 2n$ where n=odd (e.g. 200)
$\mathbf{F} = 4(f_A + f_B)$ if h, k, l all even and $h+k+l = 2n$ where n=even (e.g. 400)

CPH

Close-packed hexagonal describes a way for atoms (considered as hard spheres) to pack together to fill space. The first layer (A) consists of an hexagonal array of atoms. The next layer (B) sits in the hollows of the first layer. The third layer duplicates layer A, giving an ABAB... structure. (See fcc.)

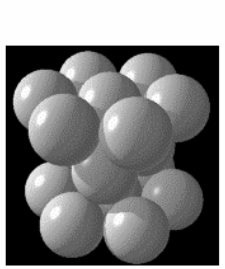

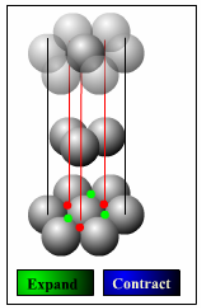

• forbidden reflections for the hcp structure occur when $h+2k = 3n$ and l is odd, where n is an integer (e.g. 113 is forbidden).

DIFFRACTION of X-rays

Experimental XRD techniques

Rotating crystal method –
for single crystals, epitaxial films
θ-2θ, rocking curve, φ - scan

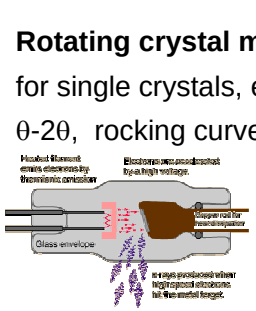

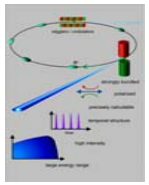

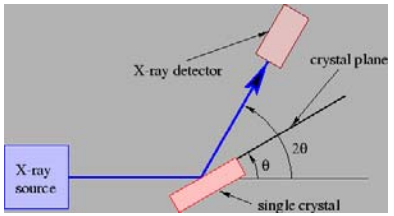

Powder diffraction

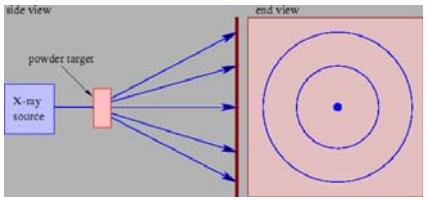

Laue method – *white* x-ray beam used most often used for mounting single crystals in a precisely known orientation

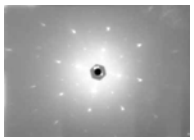

EXPERIMENTAL SETUP for Rotating Crystal Diffraction of X-rays

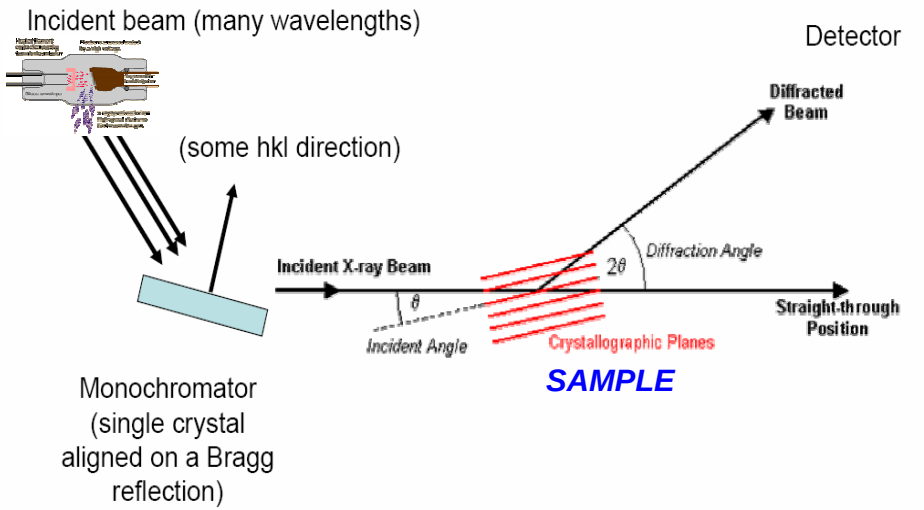

How are diffraction experiments done?

X-ray Diffraction Setup

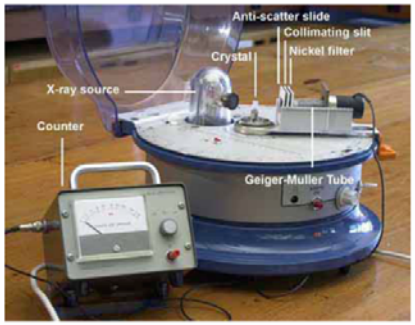

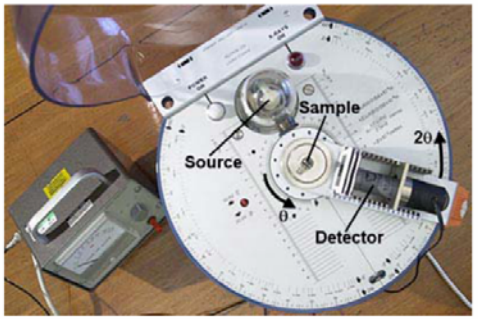

High Angular Resolution X-ray Diffraction Setup

B11 Tiernan

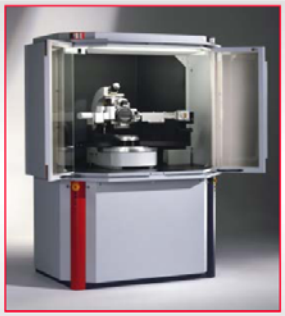

D8 Discover

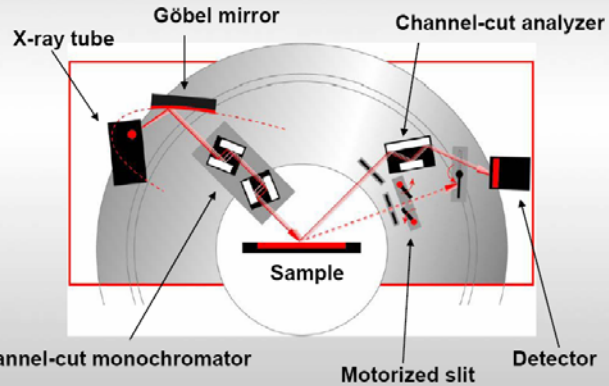

The Bragg Law

Conditions for a sharp peak in the intensity of the scattered radiation:

1) the x-rays should be specularly reflected by the atoms in one plane

2) the reflected rays from the successive planes interfere constructively

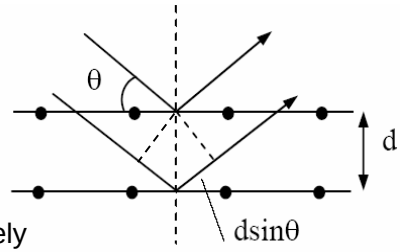

The path difference between the two x-rays: $2\mathrm{d}\cdot\sin\theta \Rightarrow$

the Bragg formula: $2\mathrm{d}\cdot\sin\theta = m\lambda$

The model used to get the Bragg law are greatly oversimplified (but it works!).

– It says nothing about intensity and width of x-ray diffraction peaks
– neglects differences in scattering from different atoms
– assumes single atom in every lattice point
– neglects distribution of charge around atoms

Diffraction condition and reciprocal lattice

Von Laue approach:

- crystal is composed of identical atoms placed at the lattice sites T
- each atom can reradiate the incident radiation in all directions.
- Sharp peaks are observed only in the directions for which the x-rays scattered from all lattice points interfere constructively.

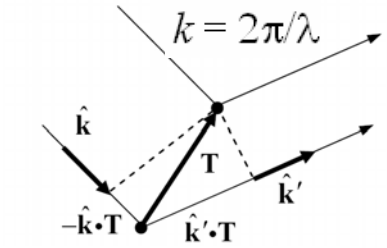

Consider two scatterers separated by a lattice vector **T**.
Incident x-rays: wavelength λ, wavevector **k**; $|\mathbf{k}| = k = 2\pi/\lambda$; $(\mathbf{k}'-\mathbf{k})\cdot\mathbf{T} = 2\pi m$
Assume *elastic* scattering: scattered x-rays have same energy (same λ) ⇒
wavevector **k'** has the same magnitude $|\mathbf{k}'| = k = 2\pi/\lambda$ $\hat{\mathbf{k}} = \frac{\mathbf{k}}{|\mathbf{k}|}$ $\hat{\mathbf{k}}' = \frac{\mathbf{k}'}{|\mathbf{k}'|}$

Condition of constructive interference: $(\hat{\mathbf{k}}'-\hat{\mathbf{k}})\cdot\mathbf{T} = m\lambda$ or

Define $\Delta\mathbf{k} = \mathbf{k}' - \mathbf{k}$ - *scattering wave vector*

Then $\Delta\mathbf{k} = \mathbf{G}$, where **G** is defined as such a vector for which $\mathbf{G}\cdot\mathbf{T} = 2\pi m$

We get $\Delta\mathbf{k} = \mathbf{k}' - \mathbf{k} = \mathbf{G} \Rightarrow |\mathbf{k}'|^2 = |\mathbf{k}|^2 + |\mathbf{G}|^2 + 2\mathbf{k}\cdot\mathbf{G} \Rightarrow G^2 + 2\mathbf{k}\cdot\mathbf{G} = 0$

$2\mathbf{k}\cdot\mathbf{G} = G^2$ – another expression for diffraction condition

We obtained the *diffraction (Laue) condition*: $\Delta\mathbf{k} = \mathbf{G}$ where $\mathbf{G}\cdot\mathbf{T} = 2\pi m$

Vectors **G** which satisfy this relation form a ***reciprocal lattice***

A reciprocal lattice is defined with reference to a particular Bravais lattice, which is determined by a set of lattice vectors **T**.

Constricting the reciprocal lattice from the direct lattice:

Let $\mathbf{a_1}, \mathbf{a_2}, \mathbf{a_3}$ - primitive vectors of the direct lattice; $\mathbf{T} = n_1\mathbf{a_1} + n_2\mathbf{a_2} + n_3\mathbf{a_3}$

Then reciprocal lattice can be generated using the primitive vectors

$$\mathbf{b}_1 = \frac{2\pi}{V}\mathbf{a}_2\times\mathbf{a}_3, \quad \mathbf{b}_2 = \frac{2\pi}{V}\mathbf{a}_3\times\mathbf{a}_1, \quad \mathbf{b}_3 = \frac{2\pi}{V}\mathbf{a}_1\times\mathbf{a}_2$$

where $V = \mathbf{a_1}\cdot(\mathbf{a_2}\times\mathbf{a_3})$ is the *volume of the unit cell*

Then vector $\mathbf{G} = m_1\mathbf{b_1} + m_2\mathbf{b_2} + m_3\mathbf{b_3}$ We have $\mathbf{b}_i\cdot\mathbf{a}_j = \delta_{ij}$

Therefore, $\mathbf{G}\cdot\mathbf{T} = (m_1\mathbf{b_1} + m_2\mathbf{b_2} + m_3\mathbf{b_3})\cdot(n_1\mathbf{a_1} + n_2\mathbf{a_2} + n_3\mathbf{a_3}) =$
$2\pi(m_1n_1 + m_2n_2 + m_3n_3) = 2\pi m$

The set of reciprocal lattice vectors determines the possible scattering wave vectors for diffraction

We got $\Delta\mathbf{k} = \mathbf{k}' - \mathbf{k} = \mathbf{G} \Rightarrow |\mathbf{k}'|^2 = |\mathbf{k}|^2 + |\mathbf{G}|^2 + 2\mathbf{k}\cdot\mathbf{G} \Rightarrow G^2 + 2\mathbf{k}\cdot\mathbf{G} = 0$

$2\mathbf{k}\cdot\mathbf{G} = G^2$ – another expression for diffraction condition

Now, show that the reciprocal lattice vector $\mathbf{G} = h\mathbf{b_1} + k\mathbf{b_2} + l\mathbf{b_3}$ is orthogonal to the plane represented by Miller indices (hkl)

plane (*hkl*) intercepts axes at points *x*, *y*, and *z* given in units a_1, a_2 and a_3

By the definition of the Miller indices:

$$(h,k,l) = \left(\frac{1}{x},\frac{1}{y},\frac{1}{z}\right)$$

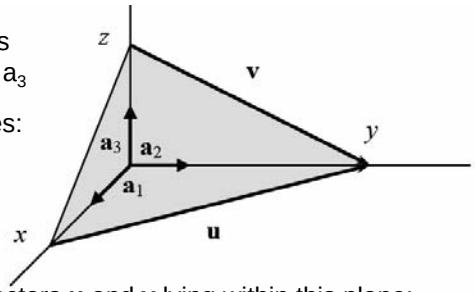

define plane by two non-collinear vectors **u** and **v** lying within this plane:

$$\mathbf{u} = y\mathbf{a}_2 - x\mathbf{a}_1 \quad \text{and} \quad \mathbf{v} = y\mathbf{a}_2 - z\mathbf{a}_3$$

prove that **G** is orthogonal to **u** and **v:**

$$\mathbf{u}\cdot\mathbf{G} = (y\mathbf{a}_2 - x\mathbf{a}_1)\cdot(h\mathbf{b}_1 + k\mathbf{b}_2 + l\mathbf{b}_3) = 2\pi(yk - xh) = 0$$

analogously show $\mathbf{v}\cdot\mathbf{G} = 0$

Now, prove that the distance between two adjacent parallel planes of the direct lattice is $d = 2\pi/G$.

The interplanar distance is given by the projection of the one of the vectors $x\mathbf{a}_1$, $y\mathbf{a}_2$, $z\mathbf{a}_3$, to the direction normal to the (*hkl*) plane, which is the direction of the unit vector $\mathbf{G}/G$

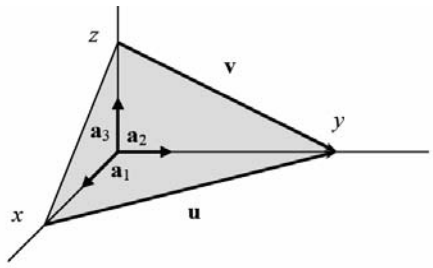

$\Rightarrow \quad d = x\mathbf{a}_1\cdot\mathbf{G}/G = 2\pi xh/G = 2\pi/G$

The reciprocal vector $\mathbf{G}(hkl)$ is associated with the crystal planes (hkl) and is normal to these planes. The separation between these planes is $2\pi/G$

$2\mathbf{k}\cdot\mathbf{G} = G^2 \Rightarrow 2|\mathbf{k}|G\sin\theta = G^2$
$\Rightarrow 2\cdot 2\pi\sin\theta/\lambda = 2\pi/d \Rightarrow 2d\sin\theta = \lambda$

$2d\sin\theta = m\lambda$ - get Bragg law

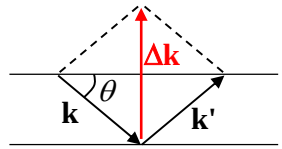

Ewald Construction for Diffraction Condition and reciprocal space

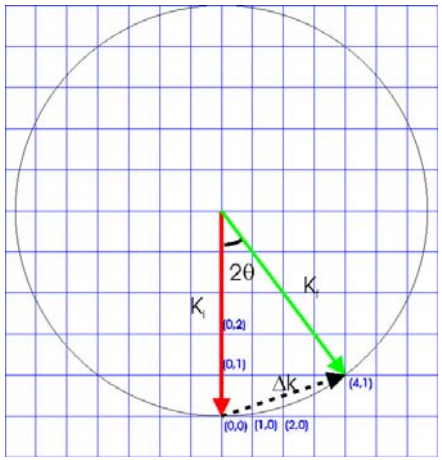

Diffraction occurs for:

$$\vec{k} + \vec{G} = \vec{k}'$$

Or

$$\vec{k}' - \vec{k} = \vec{G}$$

$$k = 2\pi/\lambda$$

Geometric interpretation of Laue condition:

$$2\mathbf{k}\cdot\mathbf{G} = G^2 \Rightarrow \quad \mathbf{k}\bullet\left(\frac{1}{2}\mathbf{G}\right) = \left(\frac{1}{2}\mathbf{G}\right)^2$$

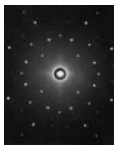

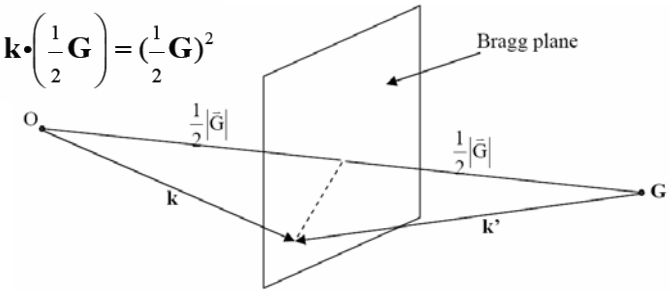

– Diffraction is the strongest (constructive interference) at the perpendicular bisecting plane (Bragg plane) between two reciprocal lattice points.

– true for any type of waves inside a crystal, including electrons.

– Note that in the original real lattice, these perpendicular bisecting planes are the planes we use to construct Wigner-Seitz cell

Geometric interpretation of Laue condition:

$$2\mathbf{k}\cdot\mathbf{G} = G^2 \Rightarrow \quad \mathbf{k}\bullet\left(\frac{1}{2}\mathbf{G}\right) = \left(\frac{1}{2}\mathbf{G}\right)^2$$

From the Laue condition, a different condition for diffraction can be derived. It is again equivalent to both Laue and Bragg.

k' - **k** = **G** and so **k'** = **G** + **k**

Taking the dot product of both sides,

(**k'** • **k'**) = (**G** + **k**) • (**G** + **k**)

Hence **k'** • **k'** = **G** • **G** + 2**G** • **k** + **k** • **k**

But the magnitudes of **k** and **k'** are equal so **k'** • **k'** and **k** • **k** cancel.

Hence 2**G** • **k** = -**G** • **G**

If there is a reciprocal lattice point at the position **G** there is also one at -**G** so the minus sign is unnecessary.

Hence **k** • ½**G** = $|\frac{1}{2}\mathbf{G}|^2$